

Nuclear Physics A610 (1996) 404c-417c

NUCLEAR PHYSICS A

Anomalous J/ ψ suppression in Pb+Pb collisions at 158×A GeV/c.

Michel Gonin⁹, for the NA50 collaboration

- M.C. Abreu⁶, C. Alexa², B. Alessandro¹¹, J. Astruc⁸, C. Baglin¹, A. Baldit⁴,
- F. Bellaiche¹², M. Bedjidian¹², S. Beole¹¹ A. Borhani⁹, V. Boldea², P. Bordalo⁶,
- A. Bussière¹, V. Capony¹, J. Castor⁴, M. Cerú³, T. Chambon⁴, B. Chaurand⁹,
- I. Chevrot⁴, B. Cheynis¹², E. Chiavassa¹¹, C. Cicalo³, S. Constantinescu²,
- W. Dabrowski¹¹, A. De Falco³ G. Dellacasa¹¹, N. De Marco¹¹, A. Devaux⁴, S. Dita²,
- O. Drapier¹², B. Espagnon⁴, J. Fargeix⁴, F. Fleuret⁹, P. Force⁴, M. Gallio¹¹,
- Y.K. Gavrilov⁷, C. Gerschel⁸, P. Giubellino¹¹, M.B. Golubeva⁷, M. Gonin⁹,
- P. Gorodetzky¹⁰, J.Y. Grossiord¹², P. Guaita¹¹, F.F. Guber⁷, A. Guichard¹²,
- R. Haroutunian¹², M. Idzik¹¹, D. Jouan⁸, T.L. Karavitcheva⁷, R. Kossakowski¹,
- L. Kluberg⁹, A.B. Kurepin⁷, Y. Le Bornec⁸, G. Landaud⁴, C. Lourenço⁵, L. Luquin⁴,
- P. Macciotta³, F. Ohlsson-Malek¹², A. Marzari-Chiesa¹¹, M. Masera¹¹, A. Masoni³,
- S. Mourgues⁴, A. Musso¹¹, P. Petiau⁹, W.L. Prado da Silva^{11a}, A. Piccotti¹¹, J.R. Pizzi¹²,
- G. Puddu³, C. Racca¹⁰, L. Ramello¹¹, S. Ramos⁶, P. Rato-Mendes¹¹, L. Riccati¹¹,
- A. Romana⁹, M.S. Sartori¹¹, P. Saturnini⁴, E. Scomparin¹¹, R. Shaoian⁵, S. Silva⁶,
- S. Serci³, P. Sonderegger⁵, X. Tarrago⁸, P. Temnikov³, N.S. Topilskaya⁷, G. Usai³,
- E. Vercellin¹¹, and N. Willis⁸.
- ¹ L.A.P.P., IN2P3-CNRS, F-74019 Annecy-le-Vieux, France
- ² I.F.A., R-76900 Bucharest, Romania.
- ³ Università di Cagliari, I.N.F.N., Cagliari, Italy.
- ⁴ L. P. C., IN2P3-CNRS, F-63177 Aubière Cedex, France
- ⁵ C.E.R.N., CH-1211 Geneva 23, Switzerland
- ⁶ L.I.P., Av. E. Garcia, 14-1, P-1000 Lisbon, Portugal
- ⁷ I.N.R., 117312 Moscow, Russia.
- ⁸ I.P.N., IN2P3-CNRS, F-91406 Orsay, France
- ⁹ Ecole Polytechnique, L.P.N.H.E, IN2P3-CNRS, F- 91128 Palaiseau, France
- ¹⁰ C.R.N., IN2P3-CNRS, F-67037 Strasbourg, France
- ¹¹ Università di Torino, I.N.F.N., I-10125 Torino, Italy
- ¹² I.P.N., IN2P3-CNRS, F-69622 Villeurbanne, France
- ^a Now at UERJ, Rio de Janeiro, Brazil

Cross sections for $J/\psi, \psi'$ and Drell-Yan production in Pb+Pb collisions at $158\times A$ GeV/c are presented and compared with results obtained by the NA38 and NA51 collaborations. The Pb+Pb data have been collected by the NA50 collaboration using the NA38 dimuon spectrometer. The Drell-Yan mechanism is found to scale as $(A_{projectile} \cdot B_{target})$ in p+B_{target} and $A_{projectile} + B_{target}$ collisions including Pb+Pb collisions. Regarding J/ψ ,

an anomalous suppression is observed in Pb+Pb collisions with respect to the suppression observed in p+B_{target}, O+B_{target} and S+U collisions. The cross section ratios $\psi'/(J/\psi)$ are similar in Pb+Pb and S+U collisions.

1. INTRODUCTION

The concept of a quark-gluon plasma (QGP) predicted for heavy ion collisions [1] has been the driving force for experimental studies of hadronic matter at high energy densities. There is no single unique signature for the QGP formation but it is expected that charmonia production will be the suitable probe for the plasma phase or deconfinement [2]; hard processes should suffer, in general, no effect by the later stage of the heavy-ion collision. At the early stage, suppression of the J/ψ and ψ ' resonances is expected from Debye screening effect in the QGP or from interaction of the charmonia state with hard gluons present in deconfined matter. Measurements of charmonia cross sections along with Drell-Yan cross sections used as reference to hadron+hadron collisions, should therefore signal the QGP formation.

To these ends a systematic measurement of J/ψ , ψ ' and Drell-Yan cross section has been performed by the NA38 collaboration using proton, oxygen and sulfur beams delivered by the CERN-SPS. The experiment started to collect data 10 years ago and announced significant suppression of charmonia in central heavy ion collision [3] as predicted for the QGP formation [4]. Alternative explanations were proposed soon afterwards based on absorption of the charmonia by nuclear matter [5]. Nowadays the overall set of extensive data collected and analysed by NA38 supports the absorption mechanism in p+B_{target}, O+B_{target} and S+U collisions. Nevertheless a large absorption cross section can be deduced from the data [6], larger than expected for J/ ψ +h inelastic cross section. Recent calculations based on the colour octet model have shown that this phenomenological absorption cross section is consistent indeed with absorption of pre-resonance states (cc̄g) in nuclear matter leading finally to a coherent description of charmonia suppression in p+B_{target}, O+B_{target} and S+U collisions [7].

The NA50 experiment is an upgraded version of the NA38 experiment for the lead beam. The data were taken in November-December 1995 at CERN with a beam momentum of 158×A GeV/c on a fixed lead target. Charmonia and Drell-Yan productions were detected via their decay into muon pairs. The centrality of the collision was obtained by simultaneous measurement of neutral transverse energy, zero degree kinetic energy for hadrons and total charged particle multiplicities.

The goal of this paper is to present a preliminary analysis of the 1995 lead run and to compare these data with the data obtained with lighter projectiles by the NA38 and NA51 collaborations [8]. This includes the study of high mass muon pairs with $M_{\mu+\mu-} \ge 2.9$ GeV/c² leading to charmonia and Drell-Yan cross sections.

2. EXPERIMENTAL DETAILS

The intensity of the ²⁰⁸Pb beam was typically $\simeq 3.5 \ 10^7$ particles/spill corresponding to an average of 1000 events/spill written on tape with 95% life-time for data acquisition and about $\simeq 20\%$ pile-up events. The data presented here correspond roughly to 52 million triggers, 50000 J/ ψ , 350 ψ and around 650 Drell-Yan pairs with $M_{\mu+\mu-} \ge 4.0$

 ${\rm GeV/c^2}$. These numbers represent about 85% of the full statistics. Throughout the entire data taking period target-out runs were performed for quality controls. Three triggers were implemented simultaneously in hardware for data acquisition: the dimuon (85%), the beam (12%) and the laser (3%) trigger. The first trigger requires two muons in the spectrometer while the second requires a Pb-ion or fragment in the zero degree hadron calorimeter and is used for minimum bias event selection. The third trigger is used for quality controls.

2.1. Beam and vertex identification

A set of beam detectors made of 16 quartz blades was placed 25 meters upstream from the target providing the luminosity for the analysis and precise timing for the trigger. Interactions of the incoming Pb beam in the beam detectors and windows of the beam pipe were detected by scintillator detectors placed off the beam axis. The total thickness for the Pb target was 7 mm corresponding to a nuclear interaction length of the order of 17 %. Due to the significant interaction length, the target was divided in 7 subtargets for identification of re-interaction of Pb fragments. Primary and secondary vertex identification was provided by quartz blades located off the beam axis. Note that the first sub-target was larger in diameter than the others in order to check that the Pb beam was totally intercepted by the sub-targets. A set of 4 quartz halo detectors placed in front of the targets were used to check the beam optics during the run and to reject beam halo for analysis.

2.2. Muon spectrometer

The NA50 experiment has used the NA38 spectrometer. In order to improve the mass resolution in NA50, the current in the magnet was increased from 4000 A to 7000 A. The mass resolution for the J/ ψ was $\sigma/M=3.3$ % providing better separation between the J/ ψ and ψ ' resonances. Large pion multiplicities are expected in Pb+Pb collisions which will give a substantial amount of background in the spectrometer from π and kaon decays. A BeO pre-absorber was placed in front of the big hadron absorber to reduce such background. For the J/ ψ mass region, the ratio signal/(signal+background) was of the order of 85 %.

2.3. Centrality detectors

The centrality of the Pb+Pb collision was obtained from the measurement of three observables: the neutral transverse energy given by an electromagnetic calorimeter, the total charge multiplicity detected with a silicon strips detector and the kinetic energy of the beam fragments determined from a zero degree hadron calorimeter. The analysis presented here uses for centrality cuts the neutral transverse energy corresponding to $E_T = E_{\pi^0} \cdot \sin(\theta)$ where E_{π^0} stands for the total energy of the produced pions and θ their polar angles. The electromagnetic calorimeter is made of scintillating fibers embedded in lead and segmented in six sextants sub-divided in four sectors. The neutral transverse energy has been measured in the pseudo-rapidity interval $1.1 < \eta < 2.3$. Contamination of charged particles was estimated and corrected based on Monte-Carlo simulations. Note that the values for the neutral transverse energy in NA50 can not be compared directly with NA38 values due to differences in the acceptance.

3. DATA ANALYSIS

The kinematical domain for the detected muon pairs is $2.93 \le y \le 3.93$ for the rapidity corresponding to $0.\le y \le 1.0$ in the center of mass system, and $-0.5 \le \cos(\theta) \le +0.5$ for the polar decay angle in the Collins-Soper reference frame. The dimuon mass spectrum was analysed for $M_{\mu+\mu-} \ge 2.9$ GeV/c² in order to reduce the charm contributions from open charm decays. The spectrometer acceptance for transverse momenta covers the full phase space.

Several cuts were applied to the data for identification of clean events. These software cuts reject events characterized by at least two incoming Pb ions within a 15 ns gate (pile-up), interaction in or near the beam detectors, beam halo and re-interaction in the sub-targets. Correction to the luminosity was made on a run by run basis. The tracking algorithm which requires exactly two muon tracks in the acceptance of the spectrometer rejects a substantial amount of false triggers, i.e. 55 % of the total number of events written on tape.

3.1. Dimuon spectra

The like-sign mass spectra are fitted with the superposition of four contributions: J/ψ , ψ , Drell-Yan and the combinatorial background.

$$\frac{dN^{+-}}{dM_{\mu\mu}} = A_{J/\psi} \cdot \frac{dN^{J/\psi}}{dM_{\mu\mu}} + A_{\psi'} \cdot \frac{dN^{\psi'}}{dM_{\mu\mu}} + A_{DY} \cdot \frac{dN^{DY}}{dM_{\mu\mu}} + \frac{dN^{Bckg}}{dM_{\mu\mu}}$$
(1)

As already mentioned, the background originates from π and kaon decays and is totally determined using the like-sign sample of the muon pairs and the well known formula assuming independent and poissonian distributions. The shape of the distributions for J/ψ , ψ 'and Drell-Yan is obtained from Monte-Carlo simulations where analytical functions were used to smooth the reconstructed simulated events. The functions can be seen on Fig.1 represented by solid lines. The overall fit to the spectra were performed by the maximum likelihood procedure for the determination of $A_{J/\psi}$, $A_{\psi'}$ and A_{DY} . The number of events for each process was obtained by integration of these three parameters. Note that for the full statistics sample, i.e. without centrality cut, the fit was performed with five free parameters including the three parameters $A_{J/\psi}$, $A_{\psi'}$, A_{DY} and the mass and width of the "gaussian-like" distribution for J/ψ . The mass for ψ' was fixed according to the mass difference between the two resonances listed in the particle data book [9]. The width for ψ' was fixed according to the width difference between the two resonances obtained from Monte-Carlo simulations.

3.2. Cross section

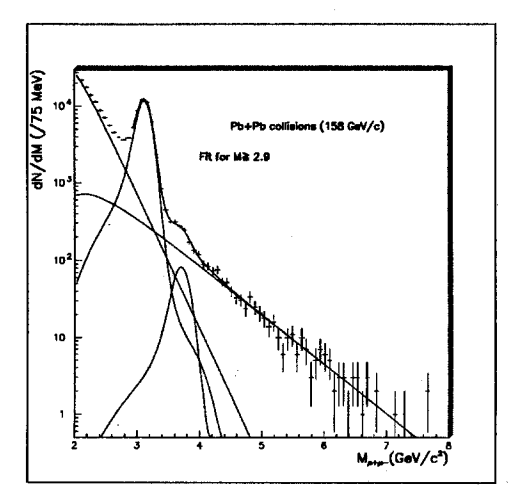
The cross section σ is defined as

$$\sigma \cdot \mathcal{L} = \frac{N^{\text{events}}}{\mathcal{A}} \tag{2}$$

where N^{events} stands for the number of J/ ψ or ψ ' or Drell-Yan pairs, \mathcal{A} the acceptance of the NA50 spectrometer and \mathcal{L} the luminosity,

$$\mathcal{L} = c \cdot N^{\text{Pb}} \cdot \epsilon_{\text{Target}} \cdot \epsilon_{\text{L.T.}} \cdot \epsilon_{\text{Recons.}} \cdot \epsilon_{\text{Trig.}} \cdot \Sigma_{\text{Pileup}} \cdot \Sigma_{\text{Halo}} \cdot \Sigma_{\text{Paras}} \cdot \Sigma_{\text{Re-int.}}$$
(3)

where N^{Pb} is the number of incoming Pb, ϵ the efficiencies and Σ the corrections needed for the different experimental cuts. The cross sections were calculated for the seven subtargets and by using only the first larger sub-target. The two procedures are in agreement within systematic errors.



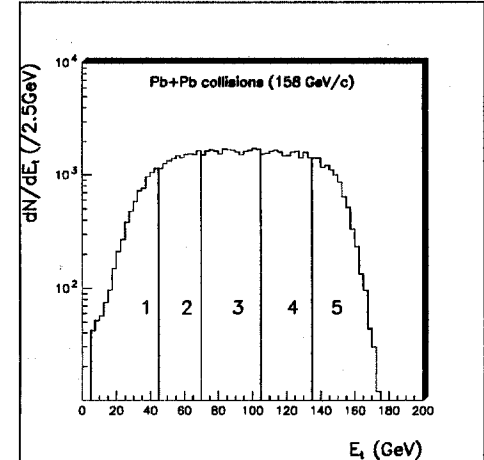


Figure 1. Opposite-sign mass distribution Figure 2. Neutral transverse energy distriin Pb+Pb collisions. See text.

bution. Centrality intervals are shown.

3.3. Efficiencies, corrections and systematic errors

The efficiencies and corrections needed for the estimate of cross sections are listed in table 1. The total systematic errors for the NA50 experiment is obtained by assuming that all the errors listed in table 1 are incoherent. The parameter ϵ_{Target} represents the efficiency for the vertex determination, $\epsilon_{L.T.}$ the life time efficiency for acquisition of the data, $\epsilon_{Rec.}$ the tracking efficiency, $\epsilon_{Trig.}$ the trigger efficiency, Σ_{Pileup} the correction for pile-up, Σ_{halo} the correction for beam halo, Σ_{Paras} the correction for interaction in beam detector and $\Sigma_{Re-interaction}$ the correction for re-interaction in the sub-targets.

3.4. Energy and isospin corrections

A large fraction of the Pb+Pb data quoted in this report are noted as "rescaled data to 200 GeV/c". For comparison of NA50 results with NA38 results, the J/ ψ data obtained at 158×A GeV/c were scaled up to 200×A GeV/c according to the simple parametrization [10]

$$\sigma = \sigma_0 \cdot (1 - M_{\mu\mu} / \sqrt{s})^{12} \tag{4}$$

where \sqrt{s} stands for the center of mass energy per nucleon. In Fig. 4, the J/ ψ cross section for Pb+Pb was multiplied by 1.32 for energy correction. The energy dependence

Table 1

Efficiencies (%) and correction (%) for cross section calculations	S
$\mathcal{A}(\mathrm{J}/\psi,\psi',\mathrm{Drell-Yan})$	13.4,15.8,14.7
ϵ_{Target}	81 ± 3
$\epsilon_{L.T.}$	96 ± 1
$\epsilon_{Reconstruction}$	95 ± 2
$\epsilon_{Trig.}$	100 + 0 - 5
Σ_{Pileup}	80 ± 1
Σ_{Halo}	97 ± 1
Σ_{Paras}	98 ± 0.5
$\Sigma_{Re-interaction}$	98 ± 0.5
total systematic errors	7 %

for Drell-Yan was given by analytical calculations at leading order using GRV-LO [11] structure functions.

References to hadron+hadron collisions were obtained with the aid of p+p and p+d results from the NA51 collaboration. This collaboration used the NA38 spectrometer to study isospin symmetry breaking in the light quark sea of the nucleon for the Drell-Yan process at 450 GeV/c [12]. We used here by-products of this experiment such as Drell-Yan and J/ ψ absolute cross sections. Data obtained for p+Cu and p+W collisions performed both at 450 GeV/c and 200 GeV/c were used to account for energy dependence and for small differences in the kinematical domains.

Corrections regarding the number of neutrons and protons in each nuclei were applied when Drell-Yan cross sections are compared between different systems. In this cases, the cross section was normalized to proton + proton collisions as

$$\sigma = \frac{\sigma_{AB}^{DATA}}{\sigma_{AB}^{GRV-LO}} \cdot (A \cdot B) \cdot \sigma^{GRV-LO} pp$$
 (5)

where σ_{pp}^{GRV-LO} represents the calculated cross section for proton+proton collisions. The value σ_{AB}^{GRV-LO} is a linear combination of the elementary cross section σ_{pp}^{GRV-LO} , σ_{pn}^{GRV-LO} , σ_{np}^{GRV-LO} and σ_{nn}^{GRV-LO} . The Drell-Yan cross section for Pb+Pb was for example multiplied by 1.31 for isospin correction. This corrections were not applied to charmonia cross section since its production mechanism is dominated at low X_F by gluon fusion when compared with quark annihilation.

3.5. Centrality cuts and average length (L) of the path of the charmonia

For J/ψ cross section studies, the data sample were divided in five neutral transverse energy intervals. This can be seen on Fig.2 where the transverse energy distribution for events with $M_{\mu+\mu-} \ge 2.0 \text{ GeV/c}^2$ (not corrected for background) is displayed. Note that this distribution is not corrected for vertex determination efficiencies. The average values and the corresponding impact parameter calculated from these values using the wounded nucleons procedure are presented in table 1. For ψ ' analysis, the number of centrality intervals was reduced to four due to lower statistics.

Contrainty cuts					
	ψ		ψ'		
	$\langle \text{Et} \rangle (GeV)$	 (fm)	$\overline{<\!\operatorname{Et}\!>(GeV)}$	$\langle b \rangle (fm)$	
bin 1	35	8.3	51	7.4	
bin 2	59	6.8	84	5.3	
bin 3	88	5.0	115	3.6	
bin 4	120	3.3	144	2.0	
bin 5	149	1.8			

Table 2 Centrality cuts

In the framework of the absorption model for particles passing through nuclear matter, the survival probability can be written as

$$P = c \cdot e^{-(\rho_0 \cdot L \cdot \sigma_{absorption})} \tag{6}$$

where ρ_0 stands for the nuclear density, $\sigma_{absorption}$ the inelastic cross sections for X+nucleon collisions and L the average length of the path of the particle in nuclear matter [6]. It should be noticed that L represents for the charmonia the sum of the average length for the pre-resonance state and the fully formed colorless state. In fact, $\sigma_{absorption}$ is expected to be quite different for these two contributions [2].

4. Drell-Yan cross section

4.1. Drell-Yan process in heavy-ion collisions

The Drell-Yan mechanism in heavy – ion collisions can be considered as arising from a superposition of primary independent nucleon-nucleon collisions. Due to the small cross section $\sigma_{NN}^{D,Y}$ for the Drell-Yan mechanism in nucleon+nucleon collisions, the total cross section in $A_{projectile} + B_{target}$ collisions is given by

$$\sigma_{AR}^{D.Y.} = (A_{projectile} \cdot B_{target}) \ \sigma_{NN}^{D.Y.} \tag{7}$$

where $A_{projectile}$ and B_{target} are the atomic mass numbers of the projectile and target respectively. Hard processes such as Drell-Yan scale in heavy-ion collisions as the number of nucleon-nucleon collisions. It has been shown that **open** charm production (D-mesons) shows a mass dependence similar to the Drell-Yan production [15]. Note that for p+ B_{target} and $\pi+B_{target}$ experiments, the mass dependence was parametrized as

$$\sigma_{hB}^{D.Y.} = B_{target}^{\alpha} \cdot \sigma_{NN}^{D.Y.}. \tag{8}$$

The data give the value $\alpha = 1.007 \pm 0.018 \pm 0.028$ at 400 GeV/c for proton beams [13] and the value $\alpha = 0.988 \pm 0.005 \pm 0.013$ around 200 GeV/c for pion beams [14].

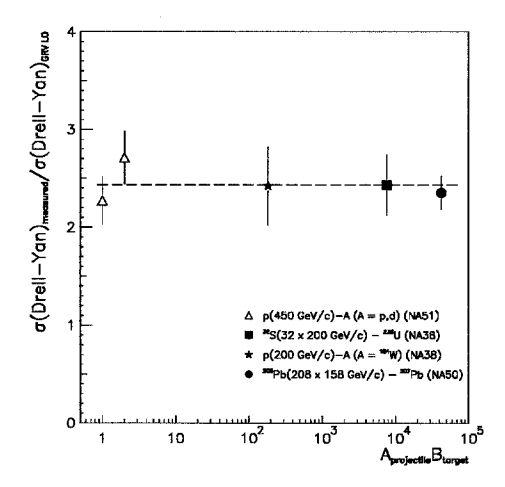
4.2. K-factors

The measured Drell-Yan cross section is $\sigma_{Pb+Pb} = 1.42 \ \mu b \pm 0.04 \pm 0.10$ for Pb+Pb collisions at 158×A GeV/c with $M_{\mu+\mu-} \ge 2.9$ GeV/c². The theoretical calculation mentioned in section 3.4 was used to compare this value with p+p, p+B_{target} and S+U values using the well known K-factor,

$$K = \frac{\sigma_{D,Y}}{\sigma_{D,Y}^{GRV-LO}} \quad . \tag{9}$$

This procedure allows direct comparisons between the different systems. The K values are shown in Fig.3. As can be seen the value for p+p, p+d, p+W, S+U and Pb+Pb are compatible with $K \simeq 2.44$. In general, the values presented on Fig.3 are in good agreement with previous data [16], but the absolute value of K depends on the detail of the calculation such as the leading order approximation and the nature of the structure functions.

The study of Drell-Yan process for the different systems presented on Fig.3 was made first to ensure that in NA50 the efficiencies and corrections needed for relation (3) are fully understood. Furthermore the data establish unambiguously that no difference is observed for hard processes such as Drell-Yan between asymmetric and symmetric systems and that relation (7) remains valid for very heavy systems.



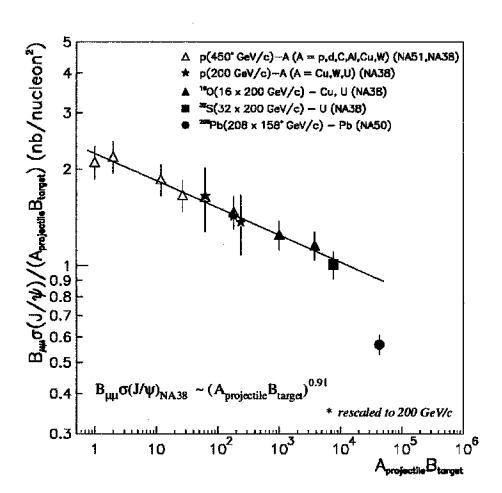


Figure 3. K-factor measured in NA51, NA38 and NA50 experiments

Figure 4. J/ψ cross sections divided by $(A_{projectile}B_{target})$ and measured in NA51, NA38 and NA50 experiments.

5. J/ψ cross section

The measured J/ ψ cross section times branching ratio to muon pairs is $B\sigma_{Pb+Pb}=19.0$ μ b \pm 0.20 \pm 1.4 for Pb+Pb collisions at 158×A GeV/c. This result is compared in Fig.4 with a systematic of the NA38 and NA51 results. The data on this figure are divided by ($A_{projectile} \times B_{target}$) which is taken as a reference to the number of nucleon+nucleon collisions for the different systems.

The nuclear dependence for charmonia production in $A_{projectile} + B_{target}$ collisions is parametrized as

$$\sigma_{AB}^{J/\psi} = (A_{projectile} \cdot B_{target})^{\alpha} \cdot \sigma_{NN}^{J/\psi} \tag{10}$$

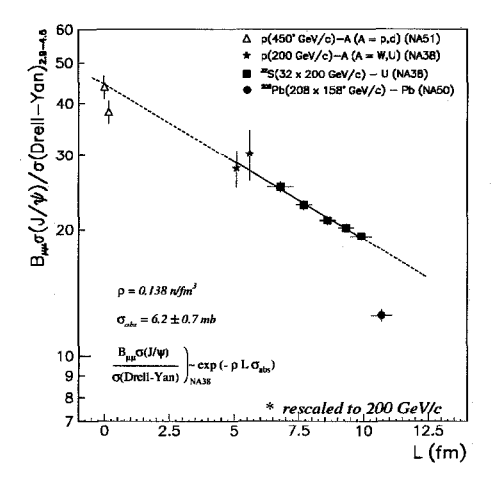
Early experiments have observed "nuclear effects" for the J/ ψ production; the α value was found to be significantly different from one. Near 200 GeV/c and for kinematical domains similar to NA50, the values deduced are $\alpha=0.96\pm0.01$ using pion beams and $\alpha=0.93\pm0.03$ using proton beams [17]. At Fermilab for the same kinematical domain than NA50 but at 800 GeV/c, the E772 experiment found $\alpha=0.920\pm0.008$ with proton beams [18]. In addition, they have shown X_F dependence for this value which drops to \simeq 0.80 at large X_F .

The following value $\alpha=0.91\pm0.01$ was obtained from a fit to the NA38 and NA51 data presented on Fig. 4 where the error quoted is a statistical error. This "nuclear effects" was called "J/ ψ suppression" by the NA38 collaboration. It should be pointed out that in contrast with previous experiments, this value is deduced for a wide range of projectile and target masses. Nonetheless this value is in very good agreement, better than systematic errors, with the value obtained at higher energy by E772 or by the NA3 experiment using proton beam.

As can be seen from Fig.4, the J/ψ cross section for Pb+Pb is smaller than the expected value obtained with the relation $(A_{projectile} \cdot B_{target})^{0.91}$ shown by the solid line. This result suggests an **anomalous** J/ψ suppression in Pb+Pb collisions in comparison with p+B_{target}, O+B_{target} and S+U collisions. All the data presented on Fig.4 are obtained after corrections presented in section 3 for the **same** kinematical domain.

6. $(J/\psi)/(Drell-Yan)$ cross section ratios

As already mentioned, the Drell-Yan cross section scale as $(A_{projectile} \cdot B_{target})$ implying that the measurement of the ratio $\sigma^{J/\psi}/(A_{projectile}B_{target})$ can be replaced by the measurement of $\sigma^{J/\psi}/\sigma^{Drell-Yan}$. An important difference for the $\sigma^{J/\psi}/\sigma^{Drell-Yan}$ ratios is that they are free from luminosity normalization errors. Fig. 5 shows the cross section ratios versus the average length L. Errors presented on this figure are statistical errors only. The lack of data points in Fig.5 with respect to Fig.4 is due poor statistics for the Drell-Yan mechanism for the missing data. The data sample for S+U are divided on this figure in five centrality intervals using neutral transverse energy measurement. It should be noted that Fig.5 confirms the anomalous suppression shown in Fig. 4 obtained with absolute cross section. In the framework of the absorption model, the cross section for dissociation of the $(c\bar{c})$ pair by nucleon is $\sigma_{absorption} = 6.2 \pm 0.7$ mb. This value is obtained from the fit of the NA38 data and shown by a full line on Fig.4. The NA51 data points



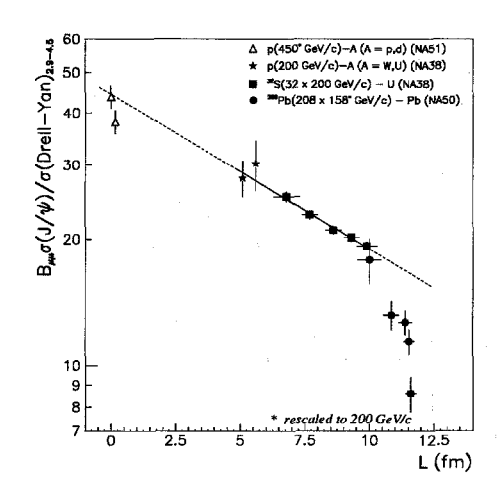


Figure 5. Cross section ratios versus the average length L of the path in nuclear matter.

Figure 6. Cross section ratios versus L for five centrality intervals in Pb+Pb.

are not included in the fit and are shown as reference to hadron+hadron collisions only. As can be seen from this figure and in contrast with NA38 data, the suppression of J/ψ in Pb+Pb collisions cannot be explained by nuclear absorption only.

In order to estimate quantitatively the anomalous J/ψ suppression, the ratio r_k was defined as

$$r_{k} = \frac{(\sigma^{J/\psi}/\sigma^{Drell-Yan})_{measured}}{(\sigma^{J/\psi}/\sigma^{Drell-Yan})_{absorption}}$$
(11)

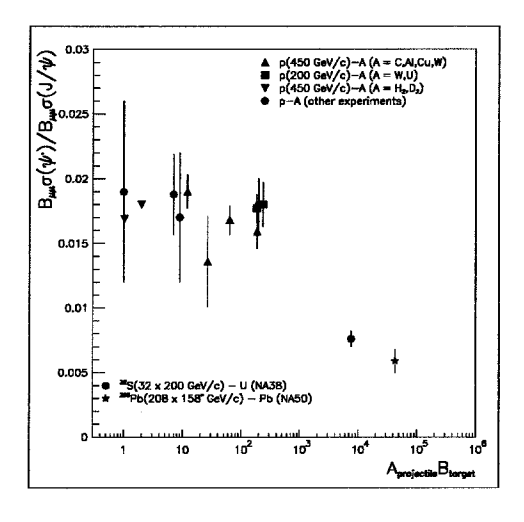
where $(\sigma^{J/\psi}/\sigma^{Drell-Yan})_{absorption}$ stands for the expected Pb+Pb value from the full line drawn in figure 5. The data give the following value

$$r_k = 0.71 \pm 0.03$$
 (12)

The measured value lies 10 standard deviations below the expected nuclear absorption value.

The detailed variation of the cross section ratios versus L is displayed on Fig.6 for the Pb+Pb collisions. For these collisions the value of the average length L increases with centrality but reaches rapidly its geometrical limit as can be seen in Fig.6. When plotted versus L the anomalous suppression appears as a sharp discontinuity from the nuclear absorption mechanism in Pb+Pb collisions. For the lower Pb+Pb centrality bin corresponding to moderately large impact parameter the data point is fully compatible with the one obtained in S+U central collisions. This important result implies that no anomalous J/ψ suppression is observed in peripheral (b \geq 8 fm) Pb+Pb collisions. This

is not the case for more central Pb+Pb collisions where anomalous suppression keeps increasing. The value r_k drops to (0.52 ± 0.05) for the most central collisions which correspond still to non zero impact parameter (b $\simeq 2$ fm).



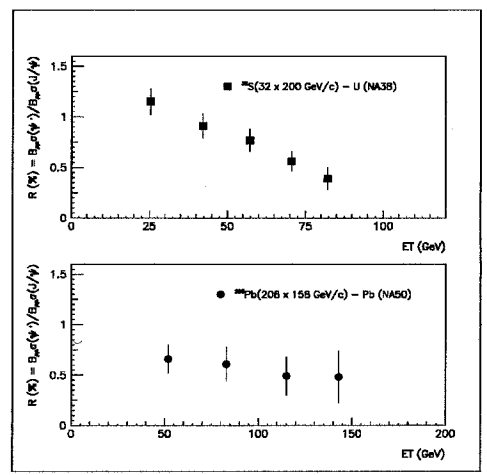


Figure 7. $\psi'/(J/\psi)$ ratios in p+B_{target}, S+U and Pb+Pb collisions

Figure 8. $\psi'/(J/\psi)$ ratios versus centrality in S+U and Pb+Pb collisions

7. $\psi'/(J/\psi)$ cross section ratios

This section begins with preliminary remarks regarding the analysis of ψ ' production. In contrast with J/ψ and Drell-Yan analysis, the cross section for ψ ' was obtained by including an open charm contribution to the different contributions for the opposite-sign mass spectra. Relation (1) was modified to

$$\frac{dN^{+-}}{dM_{\mu\mu}} = A_{J/\psi} \cdot \frac{dN^{J/\psi}}{dM_{\mu\mu}} + A_{\psi'} \cdot \frac{dN^{\psi'}}{dM_{\mu\mu}} + A_{DY} \cdot \frac{dN^{DY}}{dM_{\mu\mu}} + \frac{dN^{D\bar{D}}}{dM_{\mu\mu}} + \frac{dN^{Bckg}}{dM_{\mu\mu}}$$
(13)

where $dN^{D\bar{D}}$ represents the charm contribution obtained from p+B_{target} extrapolations [19]. The effect of the open charm contribution to the ratio $\psi'/(J/\psi)$ is about 8%. Unlike J/ψ and Drell-Yan absolute cross section, the ratio $\psi'/(J/\psi)$ was taken to be independent of the beam energy as shown by Fermilab experiments [20]. Therefore no rescaling factor was applied for comparison between NA38 and NA50 data. Finally it should be pointed out that errors quoted in this section are statistical errors only and that estimation of systematic errors are still on progress.

Due to different binding energies between the two charmonia, the ψ ' production in p+B_{target} and A_{projectile} + B_{target} collisions provides a useful comparison with J/ ψ production. In particular the cross section ratios will constrain any theoretical work regarding

the J/ ψ suppression in heavy-ion collisions. In the framework of the absorption model for example, the dissociation cross section should be larger for ψ ' than for J/ ψ leading to greater suppression of ψ ' relative to J/ ψ as a function of the centrality of the collision.

A compilation of $\psi'/(J/\psi)$ ratios for p+B_{target}, S+U and Pb+Pb is displayed in Fig.7. As already pointed out by several authors, this ratio is independent of the target mass for p+B_{target} collision; the same amount of suppression for the two charmonia is observed for these collisions. This is not the case for S+U collisions where greater suppression of ψ' relative to (J/ψ) is observed. As can be seen from Fig.7, the ratio $\psi'/(J/\psi)$ in Pb+Pb collisions is compatible within errors with the ratio obtained in S+U collisions, i.e. (0.76 ± 0.06) % for S+U collisions and (0.59 ± 0.09) % for Pb+Pb collisions. The suppression of ψ' relative to (J/ψ) stops to increase in Pb+Pb collisions relative to S+U collisions. Nevertheless it is worthwhile to point out that this is true for the ratio only but not for the absolute ψ' production normalized to the number of nucleon+nucleon collisions. The ratio $\psi'/(D\text{rell-Yan})$ can be written as

$$\frac{B\sigma^{\psi'}}{\sigma^{Drell-Yan}} = \frac{B\sigma^{\psi}}{B\sigma^{\psi}} \cdot \frac{B\sigma^{\psi}}{\sigma^{Drell-Yan}} \quad , \tag{14}$$

and from the values shown Fig.4 and. Fig.7 we deduced

$$\left(\frac{B\sigma^{\psi'}}{\sigma^{Drell-Yan}}\right)_{Pb+Pb} = \left(0.46 \pm 0.08\right) \cdot \left(\frac{B\sigma^{\psi'}}{\sigma^{Drell-Yan}}\right)_{S+U} \tag{15}$$

for the comparison of ψ ' production between Pb+Pb and S+U collisions. In conclusion, the result shown in Fig.7 for the two heavy systems seems to be due to the anomalous J/ψ suppression shown on Fig.6 rather than a saturation in the ψ ' suppression in Pb+Pb collisions.

The trend of the ψ ' suppression relative to ψ as a function of centrality seems to be different in Pb+Pb collisions with respect S+U collisions. This can be seen on Fig.8 where the cross section ratios are plotted as a function of the neutral transverse energy. In contrast with S+U results, the Pb+Pb data points seem to be independent of the centrality of the collision although these figures should be taken as indicative rather than conclusive. Relation (15) and Fig.6 suggest that this behavior is due to the sharp decrease of J/ ψ versus centrality shown on Fig.6 rather than a saturation of ψ ' suppression versus centrality. In other words, in Pb+Pb collisions J/ ψ is suppressed versus centrality by the same amount than ψ ' while in S+U collisions the J/ ψ suppression was less pronounced than the ψ ' suppression.

8. Summary and remarks

The productions of ψ , ψ ' resonances and Drell-Yan pairs have been studied for Pb+Pb collisions and a comparison has been made with p+p,p+B_{target},O+B_{target} and S+U collisions. We may summarize the results as follows:

- assuming $\alpha = 1$ for the Drell-Yan mechanism in heavy-ion collisions, identical K-factors were found for p+p, p+d, p+W, S+U and Pb+Pb collisions.
 - the J/ ψ cross section scales as $(A_{projectile} \cdot B_{target})^{\alpha}$ with $\alpha = 0.91 \pm 0.01$ in

p+B_{target}, O+B_{target} and S+U collisions.

- anomalous J/ ψ is observed in Pb+Pb collisions due to the violation of the power law ($\alpha < 0.91$).
- the value of the ratio $J/\psi/(Drell-Yan)$ lies a factor 0.71 ± 0.03 bellow the value expected from the absorption model.
- \bullet this value drops to 0.52 \pm 0.05 for central Pb+Pb collisions while no anomalous suppression is observed for Pb+Pb peripheral collisions.
- the ratio $\psi'/(J/\psi)$ in Pb+Pb collisions is compatible with the value obtained in S+U collisions.

These results are not easy to explain and it is beyond the scope of this report to speculate about the origin of the anomalous suppression observed in Pb+Pb collisions. Nonetheless it is worthwhile to notice that quantitative explanations for the anomalous suppression was proposed during this meeting [21], [22], [23]. The idea is that local energy densities should be larger in Pb+Pb than in S+U or in lighter systems. An occurrence of a new phase is supposed to take place in Pb+Pb collisions when local energy density exceeds the maximum value obtained in S+U collisions. In this new phase, the charmonia are totally [21] [22] or almost totally [23] dissociated suggesting QGP formation in central Pb+Pb collisions.

An alternative scenario was proposed based on absorption of the charmonia by "comovers" such as pions having similar rapidites than charmonia [24]. These calculations reproduce some features of the Pb+Pb results but it should be noticed that we observed a (29 ± 3) % anomalous suppression in Pb+Pb. Therefore to prove or disprove any scenario for Pb+Pb collisions, theoretical calculations should first reproduce the NA38 and NA51 data set with an **accuracy** much better than 20-30 %.

9. Acknowledgements

The collaboration NA50 would like to thank Dr. Lau Gatignon for its invaluable effort regarding our beam line optics throughout the entire data taking period.

REFERENCES

- For example, Berndt Muller, Lecture given at the NATO Advanced Study Institue, DUKE-TH-92-36.
- 2. D. Kharzeev, CERN-TH/95-342; H. Satz, CERN-TH/96-118.
- 3. NA38 collaboration, C. Baglin et al., Phys. Lett B220 (1989) 471, B251 (1990) 465.
- 4. T. Matsui and H. Satz, Phys. Lett. B178 (1986) 416.
- A. Capella et al., Phys. lett B206 (1988) 471, C. Gerschel and J. Hufner, Phys. Lett B207 (1988) 253.
- 6. C. Gerschel and J. Hufner, Z. Phys. C56 (1992) 71.
- 7. D. Kharzeev and H. Satz, CERN-TH/95-214r.
- 8. NA38 collaboration, to be published; NA51 collaboration, to be published.
- 9. Review of particles properties, Phys. Rev. D50 (1994).
- 10. G.A. Schuler, CERN-TH.7170/94.
- 11. M. Gluck, E. Reya and A. Vogt. Z. Phys. C53 (1992) 127.

- 12. NA51 collaboration, A. Baldit et al., Phys. Lett. B332 (1994) 244.
- 13. E288 collaboration, A. Ito et al., Phys. Rev. D23 (1981) 604.
- 14. NA10 collaboration, P. Bordalo et al., Phys. Lett. B193 (1994) 368 and 373.
- 15. M.J. Leitch et al., Phys, Rev, D52 (1995) 4251.
- 16. NA3 collaboration, J. Badier et al., Zeit. Phys. 11 (1981) 195 and references therein.
- 17. NA3 collaboration, J. Badier et al., Zeit. Phys. 20 (1983) 101.
- 18. E772 collaboration, D.M. Alde et al., Phys. Rev. Lett, 66 (1991) 133.
- 19. NA50 collaboration, E. Scomparin, contribution to this conference.
- 20. E789 collaboration, P.L. McGaughey, contribution to this conference.
- 21. J.P. Blaizot and J.Y. Ollitrault, Preprint Saclay T96-039.
- 22. D. Kharzeev, contribution to this conference.
- 23. C.Y. Wong, Preprint ORNL-CTP-96-07.
- 24. S. Gavin and R. Vogt, Preprint LBL 37980.